

# Type-dependent irreversible stochastic spin models for biochemical reaction networks

J. Ricardo G. Mendonça<sup>\*</sup> and Mário J. de Oliveira<sup>†</sup>

*Instituto de Física, Universidade de São Paulo – Caixa Postal 66318, 05314-970 São Paulo, SP, Brazil*

We describe an approach to model biochemical reaction networks at the level of promotion-inhibition circuitry through a class of stochastic spin models that depart from the usual chemical kinetics setup and includes spatial and temporal density fluctuations in a most natural way. A particular but otherwise generally applicable choice for the microscopic transition rates of the models also makes them of independent interest. To illustrate the formalism, we investigate some stationary state properties of the repressilator, a synthetic three-gene network of transcriptional regulators that possesses a rich dynamical behaviour.

PACS numbers: 82.39.-k, 64.60.De, 02.50.Ga

Keywords: Biochemical reaction network, stochastic spin model, lattice model, promotion-inhibition circuitry, repressilator

## I. INTRODUCTION

The modeling of biochemical reaction networks is traditionally carried out through rate equations based on techniques inherited from the field of chemical kinetics, sometimes with refinements such as the use of time-delayed terms, differential-difference equations, and stochastic perturbations [1–3]. However, the central paradigms of chemical kinetics, namely, the law of mass-action and the well-stirred reactor approximation, are valid only for slow processes occurring in dilute solutions at local equilibrium that hardly hold in the crowded cellular environment—in a typical cell, macromolecules can occupy as much as 40% of the total volume available in concentrations of 50–400 mg/ml, with steric repulsion effects contributing to the toughness of the medium [4]. Chemical master equations, a mesoscopic approach to chemical kinetics that possesses connections with several branches of nonequilibrium statistical mechanics, are also based on the well-stirred approximation [5, 6]. In order to circumvent the limitations of the rate equations and also to provide modeling tools at varied levels of abstraction, approaches based on Boolean networks, stochastic Petri nets, and rule-based formalisms, among others, have been developed [7]. While some of these approaches are innovative in proposing new forms of representing biochemical reaction networks and integrating the models with laboratory tools and automation (and, as such, sometimes are more of a metamodelling nature), most seldomly abandon chemical kinetics ideas for quantitative predictions.

Here we present an approach to the modeling of biochemical kinetic phenomena akin to stochastic spin models that seems promising [8, 9]. It can in principle represent essential features of the components of the systems more directly, providing constraints on parameters associated with behaviours that can be observed in the wet laboratory, potentially alleviating the parameter inference step that greatly hampers semi-phenomenological approaches based on rate equations [10]. The spin-like models presented here can also be explored to address the practical and difficult question of putting together

deterministic kinetics associated with continuous variables and stochastic kinetics associated with discrete variables, both of which occur in processes of biochemical interest, thus providing an alternative to the analysis of biochemical pathways where stochasticity is known to play a role [11–16].

## II. TYPE-DEPENDENT STOCHASTIC SPIN MODELS

Let  $\mathcal{T} = \{a_1, a_2, \dots, a_n\}$  be a finite set of  $n$  types (e.g., genes or proteins),  $\mathcal{S}_a = \{s_a^{(1)}, s_a^{(2)}, \dots, s_a^{(S_a)}\}$  the set of  $S_a$  possible internal states of type  $a$ , and  $\mathcal{E} = \{(a, s) : a \in \mathcal{T}, s \in \mathcal{S}_a\}$ . Also, let  $\mathcal{V}$  be the vertex set of a simple graph of order  $V = |\mathcal{V}|$ . We call the ordered pair  $(i, a) \in \mathcal{X} = \mathcal{V} \times \mathcal{T}$  a site and denote its internal state by  $\eta_i^a \in \mathcal{S}_a$ , the state space of configurations  $\boldsymbol{\eta} = (\eta_i^a)$  being given by  $\Omega = \mathcal{S}_{a_1}^{\mathcal{V}} \times \mathcal{S}_{a_2}^{\mathcal{V}} \times \dots \times \mathcal{S}_{a_n}^{\mathcal{V}}$ . Sites interact through a set of two-body interaction matrices  $J_{ij}^{ab}(\cdot, \cdot) : \mathcal{E} \times \mathcal{E} \rightarrow \mathbb{R}$ , one for each pair of positions  $i, j \in \mathcal{V}$ . Interactions between types do not need to be symmetric,  $J_{ij}^{ab} \neq J_{ji}^{ba}$ ; otherwise, we will only consider isotropic interactions,  $J_{ij}^{ab} = J_{ji}^{ab}$ . The element  $J_{ij}^{ab}(\eta_i^a, \eta_j^b)$  denotes the interaction strength that site  $(i, a)$  in the internal state  $\eta_i^a$  exerts upon site  $(j, b)$  in the internal state  $\eta_j^b$ . From these matrices we define an “energy” function  $H : \Omega \rightarrow \mathbb{R}$  as

$$H(\boldsymbol{\eta}) = \sum_{(j,b) \in \mathcal{X}} H_j^b(\boldsymbol{\eta}), \quad H_j^b(\boldsymbol{\eta}) = \sum_{(i,a) \in \mathcal{X}_j^b} J_{ij}^{ab}(\eta_i^a, \eta_j^b), \quad (1)$$

where  $\mathcal{X}_j^b$  is a neighbourhood of  $(j, b)$  that may or may not include  $j, b$ , or  $(j, b)$ . If  $\eta_i^a$  promotes  $\eta_j^b$ ,  $J_{ij}^{ab}(\eta_i^a, \eta_j^b) < 0$ , while if  $\eta_i^a$  inhibits  $\eta_j^b$ ,  $J_{ij}^{ab}(\eta_i^a, \eta_j^b) > 0$ . Viewed as a spin Hamiltonian,  $H(\boldsymbol{\eta})$  is closely related with  $N$ -colour Ashkin-Teller and Potts models [17, 18], but generalises them on the counts that it is in general a mixed-spins model, since the internal state spaces  $\mathcal{S}_a$  do not need to be all identical, and that interactions between different types do not need to be symmetric.

Function  $H(\boldsymbol{\eta})$  allows us to define a dynamics for the transitions of the internal states of the sites from the change in  $H(\boldsymbol{\eta})$  brought by the transitions, as with the usual stochastic spin models [8]. Here we will consider single-site transitions, although stirring can be added with some extra care. Let  $\boldsymbol{\eta}_i^a(s) \in \Omega$  be the configuration given by  $[\boldsymbol{\eta}_i^a(s)]_j^b = s$  if

<sup>\*</sup> Email: jricardo@if.usp.br

<sup>†</sup> Email: oliveira@if.usp.br

$(j, b) = (i, a)$  and  $[\eta_i^a(s)]_j^b = \eta_j^b$  otherwise. The energy cost of a transition  $\eta_i^a(r) \rightarrow \eta_i^a(s)$  is then given by

$$\Delta_i^a(r, s)(\boldsymbol{\eta}) = H(\boldsymbol{\eta}_i^a(s)) - H(\boldsymbol{\eta}_i^a(r)). \quad (2)$$

Because of the asymmetry in the interactions,  $\Delta_i^a(r, s)(\boldsymbol{\eta})$  decomposes into  $\Delta_i^a(r, s)(\boldsymbol{\eta} \rightarrow i) + \Delta_i^a(r, s)(\boldsymbol{\eta} \leftarrow i)$ , where

$$\Delta_i^a(r, s)(\boldsymbol{\eta} \rightarrow i) = \sum_{(j, b) \in \mathcal{X}} \left[ J_{ji}^{ba}(\eta_j^b, s) - J_{ji}^{ba}(\eta_j^b, r) \right] \quad (3)$$

collects the energy difference due to the action of the sites in  $\boldsymbol{\eta}$  upon the site  $(i, a)$  when it flips from  $\eta_i^a = r$  to  $\eta_i^a = s$ , and

$$\Delta_i^a(r, s)(\boldsymbol{\eta} \leftarrow i) = \sum_{(j, b) \in \mathcal{X}} \left[ J_{ij}^{ab}(s, \eta_j^b) - J_{ij}^{ab}(r, \eta_j^b) \right] \quad (4)$$

collects the energy difference due to the action of the site  $(i, a)$  upon the sites of  $\boldsymbol{\eta}$  when it flips from  $\eta_i^a = r$  to  $\eta_i^a = s$ . We now define a dynamics for the model specified by  $H(\boldsymbol{\eta})$  through the set of single-site transition rates

$$c_i^a(r, s)(\boldsymbol{\eta}) = \Theta(\Delta_i^a(r, s)(\boldsymbol{\eta} \rightarrow i)), \quad (5)$$

where  $\Theta : \mathbb{R} \rightarrow \mathbb{R}_+$  is any non-increasing function obeying the condition  $\Theta(\Delta)e^\Delta = \Theta(-\Delta)e^{-\Delta}$ .

The transition rates (5) depend only on the energy difference of the single site that flips, not on the global energy difference caused by the flip. From the vantage point of the flipping site, it is as if the rest of the system acted as a heat reservoir that goes unperturbed by the flip—only subsequent flips will eventually notice the change. This diverts from the usual recipe and has the important consequence that the stationary states of the model will not be distributed according to the Gibbs measure  $\mu_G(\boldsymbol{\eta}) \propto \exp(-H(\boldsymbol{\eta}))$ , although there may be some function of  $\boldsymbol{\eta}$ , different from  $H(\boldsymbol{\eta})$ , that renders a Gibbs-like stationary distribution for the model. For reversible stochastic spin models, single-site transition rates given by  $c_i^a(r, s)(\boldsymbol{\eta}) = \Theta(\Delta_i^a(r, s)(\boldsymbol{\eta}))$  guarantee that the stationary state will be distributed according to  $\mu_G(\boldsymbol{\eta})$ . For symmetric interactions,  $J_{ij}^{ab} = J_{ji}^{ba}$ , we obtain from eqs. (3) and (4) that  $\Delta_i^a(r, s)(\boldsymbol{\eta}) = 2\Delta_i^a(r, s)(\boldsymbol{\eta} \rightarrow i)$ , and the two prescriptions coincide up to a factor of 2. So, why should one pick the transition rates given by eq. (5) instead of those that guarantee that the system will relax to its equilibrium Gibbs distribution? The answer is that the rates in eq. (5) lead to forward Kolmogorov equations that, in the mean field approximation—corresponding to a well-stirred solution—and in the limit of a large number of particles are equivalent to a dynamical system  $\dot{\mathbf{x}}_t = V(\mathbf{x}_t)$  for the density profile  $\mathbf{x}_t \in \mathbb{R}^{\mathcal{X}}$ , with a smooth drift vector field  $V(\mathbf{x}_t) : \mathbb{R}^{\mathcal{X}} \rightarrow \mathbb{R}^{\mathcal{X}}$  of the form  $f(\mathbf{x}_t) - g(\mathbf{x}_t)$ . The rates given by eq. (5) are thus the ones that correctly establish the connection between the microscopic description in terms of the Markov jump process governed by  $H(\boldsymbol{\eta})$  and the macroscopic description in terms of rate equations. This result was obtained in [9] and is mildly related with results first obtained by T. Kurtz in the 1970s [19], but the introduction of the type-dependent stochastic spin models (1) and the rates (5) is novel and provides a versatile modeling framework of independent interest.

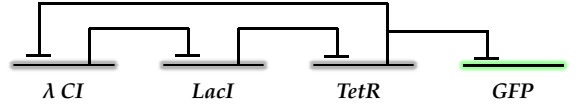


FIG. 1. The repressilator genetic regulatory network circuit. Blunt arrows indicate inhibition through a genetic regulation mechanism described in the text.

The simplest type-dependent stochastic spin model has all internal state spaces  $S_a = \{-1, +1\}$  and will be referred to as type-dependent stochastic Ising model (TDSIM). The most general interaction  $H_j^b(\boldsymbol{\eta})$  for TDSIMs is, to within an irrelevant additive constant, given by

$$H_j^b(\boldsymbol{\eta}) = \sum_{(i, a) \in \mathcal{X}_j^b} \left[ J_{ij}^{ab} \eta_i^a \eta_j^b + A_{ij}^{ab} \eta_i^a + B_{ij}^{ab} \eta_j^b \right], \quad (6)$$

where now  $J_{ij}^{ab}$ ,  $A_{ij}^{ab}$ , and  $B_{ij}^{ab}$  are scalar quantities. We remark that Ising-like Hamiltonians have already been used to model gene-gene interacting networks, but within the context of equilibrium distributions [20]. In our dynamic approach, the rates (5) are as important as  $H_j^b(\boldsymbol{\eta})$  itself. Notice also that the present approach is only barely related with the use of Ising spins to analyse consistency and monotonicity of reaction network graphs [21], although the determination of  $H_j^b(\boldsymbol{\eta})$  depends on such graphs.

### III. THE TDSIM FOR THE REPRESSILATOR

Let us illustrate the formalism by considering the repressilator, a genetic regulatory network designed to exhibit stable oscillations that are believed to be important in the determination of the circadian rhythms observed in most living organisms. The repressilator was induced in the prokaryote bacteria *Escherichia coli* through a genetically engineered plasmid, together with a reporter plasmid that expresses the green fluorescent protein (*GFP*). In this system, the protein *LacI* from *E. coli* inhibits the transcription of a second gene, *tetR* from the tetracycline-resistance transposon *Tn10*, whose protein product *TetR* inhibits the transcription of a third gene, *cl* from the  $\lambda$ -phage, whose protein *CI* inhibits the expression of *lacI*, closing the loop of negative feedback [22]. This genetic regulatory network is represented in Figure 1. This is clearly a highly stylised description of the true biochemical reaction network, that involves different operator sites, depends on how many proteins bind to the sites, and have lots of intermediate steps. It can, however, capture the essential nature of the interactions and is widely used to represent biochemical networks at a higher level of abstraction.

The TDSIM for the repressilator in the absence of external driving ( $A_{ij}^{ab} = B_{ij}^{ab} = 0$ ) has three coupling constants, one for each pair of unidirectionally interacting types, all positive and that can be taken homogeneous. Here we will take all coupling constants equal,  $J^{AB} = J^{BC} = J^{CA} = J$ , that despite being a considerable simplification of the full  $H_j^b(\boldsymbol{\eta})$  possesses a rich dynamical behaviour already in the mean field

approximation [9]. In this case, the two-body interaction term becomes

$$H_j(\eta) = J \sum_{i \in X_j} [\eta_i^A \eta_j^B + \eta_i^B \eta_j^C + \eta_i^C \eta_j^A]. \quad (7)$$

The main quantities of interest are the empirical densities

$$\rho_a^s = \frac{1}{V} \sum_{i \in \mathcal{V}} \delta(\eta_i^a, s), \quad (8)$$

where  $\delta(\cdot, \cdot)$  is the Kronecker delta symbol. For TDSIMs we can measure  $\rho_a = (1/V) \sum_{i \in \mathcal{V}} \eta_i^a$  instead, from which  $\rho_a^\pm = \frac{1}{2}(1 \pm \rho_a)$  can be easily recovered. The time evolution of these quantities in the stationary state of the model for some choices of  $J$  appears in Figure 2. All data were obtained by Monte Carlo simulations using a heat bath prescription  $\Theta(\Delta) = 1/(1 + e^{2\Delta})$  for the rates (5) in a simple square lattice of  $V = 100 \times 100$  sites with periodic boundary conditions and nearest-neighbour interactions. Notice that we include a given position in its own neighbourhood to allow for intrasite interactions between different types. One Monte Carlo step equals  $nV$  move attempts at randomly chosen sites  $(i, a)$ , where  $n$  is the number of different types in the system.

Figure 2 displays the density profiles in the nonequilibrium stationary state of the model. From that figure we clearly see that the densities of different types oscillate and are out of phase. Notice that the curves are mostly pairwise anticorrelated and that different types alternate in the peaks. The oscillations in fig. 2 are similar to the oscillations found experimentally as well as in ODE models and stochastic simulations [22, 23]. When  $J \approx 0$ , the types become independent or nearly independent and their densities fluctuate at will, so that we do not observe true oscillations. We could identify oscillations in our finite system for  $J \gtrsim 0.07$ . There is nothing special about this value, only that we can clearly observe oscillatory behaviour above it. We found that the amplitudes of the oscillations vary little in the range  $0.07 \lesssim J \lesssim 0.42$ , but decay for  $J \gtrsim 0.42$  and gets smaller as  $J$  gets larger past this point. We also found that the amplitudes of the oscillations scale like  $\sqrt{V}$ , signaling that the oscillations are spatially unsynchronised, since otherwise the amplitudes would scale like  $V$ . As a consequence, it becomes difficult to distinguish cycles or quasi-cycles out of the noise directly from the density profiles, and the analysis of correlation functions becomes preferable. This is well known from the study of population dynamics [24, 25]. We then compute the density-density time correlation functions in the stationary state,

$$C_{ab}(t) = \lim_{T \rightarrow \infty} \frac{1}{T} \int_0^T [\rho_a(t+t') - \bar{\rho}_a][\rho_b(t') - \bar{\rho}_b] dt', \quad (9)$$

and their power spectral densities

$$S_{ab}(\omega) = \frac{1}{2\pi} \int_{-\infty}^{\infty} C_{ab}(t) e^{-i\omega t} dt, \quad (10)$$

where  $\bar{\rho}_a$  and  $\bar{\rho}_b$  are the average densities of types  $a$  and  $b$  in the stationary state. In practice, the integration limits in (9)

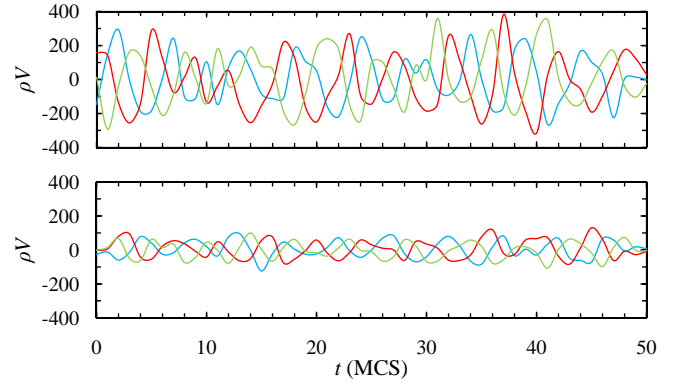


FIG. 2. Evolution of the densities of the types in the stationary state of the TDSIM for the repressilator with  $J = 0.3$  (top panel) and  $J = 0.5$  (bottom panel). The densities clearly oscillate out of phase and are pairwise anticorrelated most of the time. The oscillation amplitudes at  $J = 0.3$  are typical in the whole range  $0.07 \lesssim J \lesssim 0.42$ .

and (10) are bounded by the lengths of the time series available. In our simulations we sampled the stationary densities every  $\Delta t = \frac{1}{10}$  MCS for  $10^4$  MCS.

Figure 3 displays the autocorrelation function  $C_{AA}(t)$  at  $J = 0.415$  normalised by its value at  $t = 0$  and some associated Fourier transforms  $S_{AA}(t)$ . The other autocorrelation functions behave like  $C_{AA}(t)$  because of the symmetry between the types. We see from fig. 3 the decay of the autocorrelation function, typical of stochastic dynamics due to the variability of the oscillations, and the peak in  $S_{AA}(\omega)$  around  $\omega^* = 0.26 \pm 0.03 \text{ MCS}^{-1}$  at  $J = J^*$ . The oscillation frequencies do not vary much with  $J$  as long as  $J < J^*$ ; otherwise, the oscillations cease almost completely for  $J > J^*$ .

In Figure 4 we exhibit snapshots of the sites where  $\eta_i^a = \eta_i^b = \eta_i^c$  in the stationary state for some values of  $J$ . This figure depicts a typical transition from a disordered phase to an antiferromagnetic-like phase. We clearly see how the dynamics of the types in the stationary state becomes more and more constrained by their repressors in the immediate neighbourhood as  $J$  gets larger, hence the smaller amplitudes in the oscillations of the densities. From figs. 2 and 4 we can infer that there is a transition from a spatially uncorrelated, oscillating density stationary state to an almost frozen, non-oscillating density stationary state at  $J^* \simeq 0.415$ . The system does not freeze completely because of the frustration induced by the intrasite interactions between types and the form of the rates (5), that depend only on the single site that flips and its neighbourhood, not on the state of the entire system. We located  $J^*$  by computing the “staggered densities” in lattices of several sizes. In the dynamical mean-field approximation to the same model this transition could be identified with a Hopf bifurcation at  $J^* = 2/\cos(\pi/3) = 4$  [9]. We remark that in either case the transition at  $J^*$  should be understood as a change in the regime of the dynamical system, not as a thermodynamic phase transition, although for systems described by a function like  $H(\eta)$  the two interpretations conflate largely.

In the actual repressilator, the densities of proteins per cell oscillate with an observed period  $T_{\text{obs}} = 160 \pm 40 \text{ min}$  [22]. In

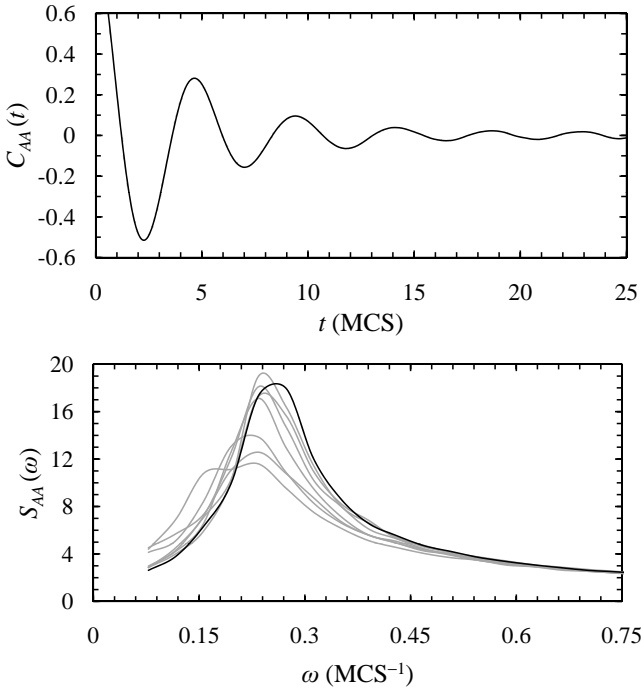


FIG. 3. Autocorrelation function  $C_{AA}(t)$  at  $J = 0.415$  normalised by its value at  $t = 0$  (upper panel) and some Fourier transforms  $S_{AA}(\omega)$  for several different values of  $0.1 \leq J \leq 0.415$  (lower panel). The curve  $S_{AA}(\omega)$  for  $J = 0.415$  (bolder line) peaks at  $\omega^* = 0.26 \pm 0.03 \text{ MCS}^{-1}$ .

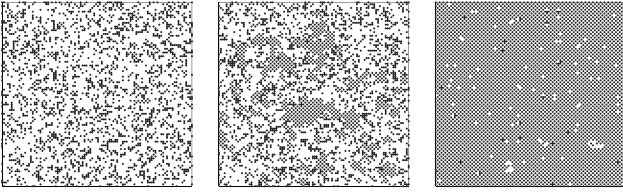


FIG. 4. Correlation between the three types in a square lattice of  $100 \times 100$  sites. The figure depicts the sites with  $\eta_i^a = \eta_i^b = \eta_i^c$  (black dots) in the stationary state when  $J = 0.3$  (left panel),  $J = 0.415$  (mid panel), and  $J = 0.5$  (right panel). At  $J = 0.5$  we see an almost exact splitting into two sublattices. In this state, the remaining dynamics, responsible for the residual small amplitude oscillations shown in the bottom panel of fig. 2, occurs mostly in the interstices between the sites with “pinned”  $\eta_i^a = \eta_i^b = \eta_i^c$ .

our simulations, we found that at  $J = J^* = 0.415$  the period  $T_{\text{sim}} = 3.9 \pm 0.4 \text{ MCS}$ . We thus have the approximate equivalence  $1 \text{ MCS} \simeq 41 \pm 7 \text{ min}$  in the real system. Translation of these figures into meaningful quantities like transcription rates is a delicate question that we intend to pursue elsewhere.

#### IV. SUMMARY AND PERSPECTIVES

Type-dependent irreversible interacting particle systems provide a tool to model the dynamics of biochemical reaction networks by linking influence flow diagrams like the one

depicted in fig. 1 with a model description at the same level of abstraction. The models can capture several characteristics of the system, are predictive, relatively simple, easily computable, and verifiable in a phenomenological sense. They can also be easily composed to describe interacting subsystems,

$$H(\eta, \xi) = H(\eta) + H(\xi) + \sum_{(j,b)} \sum_{(i,a)} K_{ij}^{ab}(\eta_i^a, \xi_j^b), \quad (11)$$

in accordance with modularity principles commended by the systems approach to biochemical reaction networks [26].

We showed that the TDSIM for the repressilator generates density oscillations that reproduce those found experimentally and in ODE-based models. To display oscillations is a non-trivial task for nonequilibrium stationary states and is only possible for TDSIMs because the rates (5) do not obey the detailed balance condition with respect to its “energy” function (1) that determines the dynamics.

The lattice structure of the spin systems provides a natural setting to study the spatiotemporal dynamics of extended networks, an aspect of biochemical reaction networks that has received increasing attention in the context of coupled gene regulatory networks [27–32]. Models can include diffusion through a Kawasaki-type exchange dynamics and also account for the possibility that types may be absent, not only inactive, in a given site, e.g., by taking some  $S_a = \{-1, 0, +1\}$ . This possibility allows the modeling of deterministic and stochastic kinetics concurrently by putting on the same model types of low density (e.g., plasmid copies or enzymes) described by discrete variables  $\eta_i^a$  together with types of higher density (e.g., peptides or small substrate molecules) described by an effective density in a mean-field-like description.

It may be that some biochemical reaction networks give rise to TDSIMs resembling Hamiltonians known from other contexts. For example, the circadian oscillations of the proteins *KaiA*, *KaiB*, and *KaiC* in cyanobacteria can be modeled by the promotion-inhibition circuit  $A \rightarrow C \dashv B \rightarrow A$  [33–35], whose TDSIM is closely related with an Ising version of the spin- $\frac{1}{2}$  ferromagnetic-ferromagnetic-antiferromagnetic trimerised Heisenberg chain [36], an important model in the study of magnetisation processes in strong fields. On the other way around, the dynamics of an activator-repressor clock model that displays both toggle switch and oscillatory behaviours [37] may be modeled by a dimerised ferromagnetic-antiferromagnetic Ising chain that seems unexplored.

We finally remark that the formalism presented here readily applies to non-biochemical reaction networks as well, providing a framework in which spatially distributed transformations are dealt with in a most natural way.

#### ACKNOWLEDGMENTS

We are indebted to Prof. Luiz Renato G. Fontes and Prof. Eduardo Jordão Neves (IME/USP) for having called our attention to TDSIMs and to Prof. Tânia Tomé (IF/USP) for helpful conversations. This work was partially supported by CNPq, Brazil, through grants PDS 151999/2010-4 (JRG) and PQ 307407/2006-3 (MJO).



- [1] P. Érdi and J. Tóth, *Mathematical Models of Chemical Reactions: Theory and Applications of Deterministic and Stochastic Models* (Princeton University Press, Princeton, 1989).
- [2] P. Schuster, "Modeling in biological chemistry. From biochemical kinetics to systems biology," *Monatsh. Chem.* **139**, 427–446 (2008).
- [3] D. T. Gillespie, "Exact stochastic simulation of coupled chemical reactions," *J. Phys. Chem.* **81**, 2340–2361 (1977); "Stochastic Simulation of chemical kinetics," *Annu. Rev. Phys. Chem.* **58**, 35–55 (2007); C. V. Rao and A. P. Arkin, "Stochastic chemical kinetics and the quasi-steady-state assumption: Application to the Gillespie algorithm," *J. Chem. Phys.* **118**, 4999–5010 (2003); D. J. Wilkinson, "Stochastic modelling for quantitative description of heterogeneous biological systems," *Nat. Rev. Genet.* **10**, 122–133 (2009).
- [4] K. Luby-Phelps, "Cytoarchitecture and physical properties of cytoplasm: Volume, viscosity, diffusion, intracellular surface area," *Int. Rev. Cytol.* **192**, 189–221 (2000); R. J. Ellis, "Macromolecular crowding: obvious but underappreciated," *Trends Biochem. Sci.* **26**, 597–604 (2001); J. A. Dix and A. S. Verkman, "Crowding effects on diffusion in solutions and cells," *Ann. Rev. Biophys.* **37**, 247–263 (2008).
- [5] D. A. McQuarrie, "Stochastic approach to chemical kinetics," *J. Appl. Probab.* **4**, 413–478 (1967).
- [6] H. Qian, "Cellular biology in terms of stochastic nonlinear biochemical dynamics: Emergent properties, isogenetic variations and chemical system inheritability," *J. Stat. Phys.* **141**, 990–1013 (2010); "Nonlinear stochastic dynamics of mesoscopic homogeneous biochemical reaction systems—an analytical theory," *Nonlinearity* **24**, R19–R49 (2011).
- [7] H. de Jong, "Modeling and simulation of genetic regulatory systems: A literature review," *J. Comput. Biol.* **9**, 67–103 (2002); J. Fisher and T. A. Henzinger, "Executable cell biology," *Nat. Biotech.* **25**, 1239–1249 (2007); G. Karlebach and R. Shamir, "Modelling and analysis of gene regulatory networks," *Nat. Rev. Mol. Cell Biol.* **9**, 770–780 (2008).
- [8] J. Marro and R. Dickman, *Nonequilibrium Phase Transitions in Lattice Models* (Cambridge University Press, Cambridge, 1999).
- [9] R. Fernández, L. R. Fontes, and E. J. Neves, "Density-profile processes describing biological signaling networks: Almost sure convergence to deterministic trajectories," *J. Stat. Phys.* **136**, 875–901 (2009).
- [10] H. W. Engl, C. Flamm, P. Kügler, J. Lu, S. Müller, and P. Schuster, "Inverse problems in systems biology," *Inverse Probl.* **25**, 123014 (2009).
- [11] H. H. McAdams and A. Arkin, "Stochastic mechanisms in gene expression," *Proc. Natl. Acad. Sci. USA* **94**, 814–819 (1997); H. H. McAdams and A. Arkin, "It's a noisy business! Genetic regulation at the nanomolar scale," *Trends Genet.* **15**, 65–69 (1999).
- [12] M. B. Elowitz, A. J. Levine, E. D. Siggia, and P. S. Swain, "Stochastic gene expression in a single cell," *Science* **297**, 1129–1131 (2002).
- [13] J. Paulsson, "Summing up the noise in gene networks," *Nature* **427**, 415–418 (2004).
- [14] J. M. Raser and E. K. O'Shea, "Control of stochasticity in eukaryotic gene expression," *Science* **304**, 1811–1814 (2004); J. M. Raser and E. K. O'Shea, "Noise in gene expression: Origins, consequences, and control," *Science* **309**, 2010–2013 (2005).
- [15] M. Kaern, W. Blake, T. C. Elston, and J. Collins, "Stochasticity in gene expression: From theories to phenotypes," *Nat. Rev. Genet.* **6**, 451–464 (2005).
- [16] E. M. Ozbudak, M. Thattai, I. Kurtser, A. D. Grossman, and A. van Oudenaarden, "Regulation of noise in the expression of a single gene," *Nat. Genet.* **31**, 69–73 (2002); A. Raj and A. van Oudenaarden, "Nature, nurture, or chance: Stochastic gene expression and its consequences," *Cell* **135**, 216–226 (2008).
- [17] J. Ashkin and E. Teller, "Statistics of two-dimensional lattices with four components," *Phys. Rev.* **64**, 178–184 (1943); C. Fan, "Symmetry properties of the Ashkin-Teller model and the eight-vertex model," *Phys. Rev. B* **6**, 902–910 (1972); G. S. Grest and M. Widom, "*N*-color Ashkin-Teller model," *Phys. Rev. B* **24**, 6508–6515 (1981).
- [18] R. B. Potts, "Some generalized order-disorder transformations," *Proc. Camb. Phil. Soc.* **48**, 106–109 (1952); F. Y. Wu, "The Potts model," *Rev. Mod. Phys.* **54**, 235–268 (1982).
- [19] T. G. Kurtz, "Solutions of ordinary differential equations as limits of pure jump Markov processes," *J. Appl. Probab.* **7**, 49–58 (1970); "Limit theorems for sequences of jump Markov processes approximating ordinary differential processes," *J. Appl. Probab.* **8**, 344–356 (1971); "The relationship between stochastic and deterministic models of chemical reactions," *J. Chem. Phys.* **57**, 2976–2978 (1972).
- [20] A. M. Walczak and P. G. Wolynes, "Gene-gene cooperativity in small networks," *Biophys. J.* **96**, 4525–4541 (2009).
- [21] E. D. Sontag, "Monotone and near-monotone biochemical networks," *Syst. Synth. Biol.* **1**, 59–87 (2007); G. Iacono and C. Altafini, "Monotonicity, frustration, and ordered response: An analysis of the energy landscape of perturbed large-scale biological networks," *BMC Syst. Biol.* **4**, 83 (2010).
- [22] M. B. Elowitz and S. Leibler, "A synthetic oscillatory network of transcriptional regulators," *Nature* **403**, 335–338 (2000).
- [23] B. Novák and J. J. Tyson, "Design principles of biochemical oscillators," *Nat. Rev. Mol. Cell Biol.* **9**, 981–991 (2008); J. J. Tyson, R. Albert, A. Goldbeter, P. Ruoff, and J. Sible, "Biological switches and clocks," *J. R. Soc. Interface* **5**, S1–S5 (2008); O. Purcell, N. J. Savery, C. S. Grierson, and M. di Bernardo, "A comparative analysis of synthetic genetic oscillators," *J. R. Soc. Interface* **7**, 1503–1524 (2010).
- [24] R. M. Nisbet and W. S. C. Gurney, *Modelling Fluctuating Populations* (Wiley, New York, 1982).
- [25] E. Arashiro, A. L. Rodrigues, M. J. de Oliveira, and T. Tomé, "Time correlation function in systems with two coexisting biological species," *Phys. Rev. E* **77**, 061909 (2008); T. Tomé and M. J. de Oliveira, "Role of noise in population dynamics cycles," *Phys. Rev. E* **79**, 061128 (2009).
- [26] L. H. Hartwell, J. J. Hopfield, S. Leibler, and A. W. Murray, "From molecular to modular cell biology," *Nature* **402**, C47–C52 (1999); M. A. Savageau, "Design principles for elementary gene circuits: Elements, methods, and examples," *Chaos* **11**, 142–159 (2001); N. Kashtan and U. Alon, "Spontaneous evolution of modularity and network motifs," *Proc. Natl. Acad. Sci. USA* **102**, 13773–13778 (2005); G. P. Wagner, M. Pavlicev, and J. M. Cheverud, "The road to modularity," *Nat. Rev. Genet.* **8**, 921–931 (2007).
- [27] D. McMillen, N. Kopell, J. Hasty, and J. J. Collins, "Synchronizing genetic relaxation oscillators by intercell signaling," *Proc. Natl. Acad. Sci. USA* **99**, 679–684 (2002).
- [28] T. S. Shimizu, S. V. Aksenov, and D. Bray, "A spatially extended stochastic model of the bacterial chemotaxis signalling

- pathway,” *J. Mol. Biol.* **329**, 291–309 (2003).
- [29] J. García-Ojalvo, M. B. Elowitz, and S. H. Strogatz, “Modelling a synthetic multicellular clock: Repressilators coupled by quorum sensing,” *Proc. Natl. Acad. Sci. USA* **101**, 10955–10960 (2004); E. Ullner, A. Zaikin, E. I. Volkov, and J. García-Ojalvo, “Multistability and clustering in a population of synthetic genetic oscillators via phase-repulsive cell-to-cell communication,” *Phys. Rev. Lett.* **99**, 148103 (2007); E. Ullner, A. Koseska, J. Kurths, E. Volkov, H. Kantz, and J. García-Ojalvo, “Multistability of synthetic genetic networks with repressive cell-to-cell communication,” *Phys. Rev. E* **78**, 031904 (2008).
- [30] M. H. Jensen, S. Krishna, and S. Pigolotti, “Repressor lattice: Feedback, commensurability, and dynamical frustration,” *Phys. Rev. Lett.* **103**, 118101 (2009).
- [31] Y. Ma and K. Yoshikawa, “Self-sustained collective oscillation generated in an array of nonoscillatory cells,” *Phys. Rev. E* **79**, 046217 (2009); W. Ye, X. Huang, X. Huang, P. Li, Q. Xia, and G. Hu, “Self-sustained oscillations of complex genomic regulatory networks,” *Phys. Lett. A* **374**, 2521–2526 (2010).
- [32] T. Danino, O. Mondragón-Palomino, L. Tsimring, and J. Hasty, “A synchronized quorum of genetic clocks,” *Nature* **463**, 326–330 (2010).
- [33] M. Ishiura, S. Kutsuna, S. Aoki, H. Iwasaki, C. R. Andersson, A. Tanabe, S. S. Golden, C. H. Johnson, and T. Kondo, “Expression of a gene cluster *kaiABC* as a circadian feedback process in cyanobacteria,” *Science* **281**, 1519–1523 (1998).
- [34] K. Kucho, K. Okamoto, Y. Tsuchiya, S. Nomura, M. Nango, M. Kanehisa, and M. Ishiura, “Global analysis of circadian expression in the cyanobacterium *Synechocystis* sp. strain PCC 6803,” *J. Bacteriol.* **187**, 2190–2199 (2005).
- [35] S. Pigolotti, S. Krishna, and M. H. Jensen, “Oscillation patterns in negative feedback loops,” *Proc. Natl. Acad. Sci. USA* **104**, 6533–6537 (2007); “Symbolic dynamics of biological feedback networks,” *Phys. Rev. Lett.* **102**, 088701 (2009).
- [36] K. Hida, “Magnetic properties of the spin-1/2 ferromagnetic-ferromagnetic-antiferromagnetic trimerized Heisenberg chain,” *J. Phys. Soc. Jpn.* **63**, 2359–2364 (1994); V. R. Ohanyan and N. S. Ananikian, “Magnetization plateaus in the ferromagnetic-ferromagnetic-antiferromagnetic Ising chain,” *Phys. Lett. A* **307**, 76–84 (2003).
- [37] M. R. Atkinson, M. A. Savageau, J. T. Myers, and A. J. Ninfa, “Development of genetic circuitry exhibiting toggle switch or oscillatory behavior in *Escherichia coli*,” *Cell* **113**, 597–607 (2003).